Constrained Layout Generation with Factor Graphs

Supplementary Material

1. Additional Experiments

1.1. Analysis of Class-wise IOU scores

In Tab. 2, the pixel-level IOU scores with macro averaging appear to be relatively low when compared to micro averaged scores. In this section, we investigate the reason for this discrepancy in scores. Macro IOU scores are computed by first calculating the class-wise IOU scores separately before averaging across each class. Therefore, we list the IOU scores for each class separately and compare them for both Graph2Plan and FP-FGNN.

The RPLAN dataset has a total of 15 classes. Tab. 5 shows the results of class-wise IOU scores for each of the 15 classes in the dataset. Firstly, for almost all the classes, FP-FGNN scores improve on Graph2Plan scores by a significant margin. The relative improvement is especially large in *DiningRoom, ChildRoom, GuestRoom* and *Storage*. However, for some of the classes like *Wall-in, Entrance* and *Exterior Wall*, the IOU scores are quite low and seems to be the primary reason for overall lower IOU-Macro score relative to IOU-Micro, since all classes are equally weighted in Macro averaging. It is worth noting that these rooms *i.e. Wall-in, Entrance* and *Exterior Wall* are mostly irregular *i.e.* not easily modeled with a bounding box and and hence, it is not surprising that the scores for these classes are lower. Additionally, bounding box for classes like *Wall-in* are usually too thin and hence, the scores are likely to be zero if the predicted box is not aligned to the same position as ground truth.

1.2. Analysis of Room overlap

One notable difference between the predicted floorplans generated by Graph2Plan and FP-FGNN is the appearance of the internal boundaries between the rooms. This is clearly visible in Fig. 3 which shows that the internal boundaries between rooms are uneven in the floorplans generated by Graph2Plan. In contrast, the floorplans generated by FP-FGNN contain straight boundaries which closely resemble the ground truth. We seek to investigate the reason for this difference, since both methods use the same CRN-based approach in generating the floorplan image from the set of bounding boxes.

One plausible reason for this difference is the amount of overlap between the predicted bounding boxes of each model. Ideally, the overlap between predicted bounding boxes should be minimal, although there may be some overlap between ground truth bounding boxes due to the non-rectangular shapes of rooms. Measuring the average overlap between predicted bounding boxes provides some information about the internal boundaries of the predicted rooms.

In Fig. 6, we show the area of intersection between each pair of predicted bounding boxes. Firstly, the average overlap area in the Ground Truth bounding boxes is 95.33. The GT box overlap area is significant since living room boxes would overlap with other rooms. FP-FGNN's average overlap area of 94.84 is similar to GT overlap and is significantly less than 112.4 of Graph2Plan, a reduction of around 18%. This supports the observation of clear and straight boundaries in floorplans generated by FP-FGNN. This reduction is likely to contribute to the clear and straight boundaries observed in the floorplans generated by FP-FGNN.

Roomtype	LivingRoom	MasterRoom	Kitchen	Bathroom	DiningRoom	ChildRoom	StudyRoom	SecondRoom
Graph2Plan	0.8593	0.8400	0.7164	0.6870	0.2018	0.4577	0.7559	0.8214
FP-FGNN	0.8470	0.9062	0.8013	0.7721	0.5743	0.8029	0.8487	0.8868
Roomtype	GuestRoom	Balcony	Entrance	Storage	Wall-in	External	ExteriorWall	
Graph2Plan	0.1433	0.7594	0.0000	0.2862	0.1303	0.9987	0.0000	
FP-FGNN	0.4193	0.8686	0.0000	0.6066	0.3822	0.9987	0.0000	

Table 5. IOU scores per each class for Graph2Plan and FGNN.

Method	Graph2Plan	FP-FGNN	GT
Average overlap	112.47	94.84	95.33

Table 6. Average area of intersection between all pairs of predicted boxes for Graph2Plan and FGNN.

Method	Box-level		Pixel-level	
	IOU - Macro	IOU - Micro	Accuracy	IOU-Micro
FP-FGNN	**0.8685**	**0.9165**	**0.8900**	**0.8017**
w/o box factors	0.7300	0.8182	0.8180	0.6923
w/o relation factors	0.8180	0.8789	0.8645	0.7609
w/o boundary factors	0.6163	0.7149	0.7903	0.6488
w/o complete factor	0.7841	0.8476	0.8473	0.7351

Table 7. Ablation study on the type of factors.

Method	Box-level		Pixel-level	
	IOU - Macro	IOU - Micro	Accuracy	IOU-Micro
FP-FGNN	**0.8685**	**0.9165**	**0.8900**	**0.8017**
w/o *inside, surrounding*	0.8481	0.9018	0.8790	0.7840
w/o *left, right*	0.8517	0.9051	0.8838	0.7918
w/o *above, below*	0.8412	0.8973	0.8804	0.7862
w/o *leftabove, leftbelow, rightabove, rightbelow*	0.8308	0.8898	0.8710	0.7710

Table 8. Ablation study on different relation factors.

Method	Box-level		Pixel-level	
	IOU - Macro	IOU - Micro	Accuracy	IOU-Micro
FP-FGNN	**0.8685**	**0.9165**	**0.8900**	**0.8017**
w/o distance feature	0.8411	0.8976	0.8831	0.7907
w/o surrounding feature	0.8333	0.8918	0.8806	0.7867

Table 9. Effectiveness of the boundary factor features.

Method	Box-level		Pixel-level	
	IOU - Macro	IOU - Micro	Accuracy	IOU-Micro
FP-FGNN(w/ Softmax)	**0.8685**	**0.9165**	**0.8900**	**0.8017**
w/ MAX	0.8436	0.8995	0.8739	0.7760
w/ SUM	0.7514	0.8272	0.8479	0.7358
w/ MEAN	0.8238	0.8848	0.8751	0.7778

Table 10. Effectiveness of the message aggregation function.

1.2.1 Ablation Studies

Different types of factors. In order to gain a better understanding of how our model functions, we study the importance of each type of factor. As shown in Tab. 7, we find that (1) every type of factor is critical and that (2) higher-order factors are more important than pairwise relation factors. Furthermore, we discover that (3) boundary factors, which capture structural constraints, are especially important. Without these boundary factors, our performance measurement, which is based on IOU-macro, experienced a significant 25% drop.

Different types of relations. To further understand our model's functioning, we conduct an ablation study on different types of relation factors. To do this, we grouped together some of the factors that capture the same constraints, such as inside and surrounding relations. Tab. 8 shows that capturing relative positional information using these factors is highly effective. Additionally, we find that each group of constraints contributes to the overall performance of our

model. These findings demonstrate the importance of carefully considering the various types of relation factors and their ability to capture critical constraints when designing and refining models for specific tasks.

Features of boundary factors. In earlier ablation studies, we discussed the critical role played by boundary factors in our model's performance, underscoring the importance of meeting structural constraints. Hence, we further investigate the different types of features we designed to capture the properties of each corner point, i.e., the distance between each corner point and the outer bounding box that encloses the boundary, and the binary boundary mask surrounding the corner point at a small offset of ϵ. As shown in Tab. 9, both features contribute to the effectiveness of the model. However, the distance feature is relatively more informative.

Message aggregation function. A crucial aspect of our message passing scheme is the message aggregator, which allows for weighted aggregation of messages using a learnable softmax-based aggregator. This function enables variables to learn from the subset of factors that are most relevant to them. To demonstrate the effectiveness of this approach, we compared our solution with three other aggregation functions: MAX, SUM, and MEAN. Our results, presented in Table 10, show that the MAX aggregator is the most effective among the three. Intuitively, MAX acts as a selection function compared to MEAN and SUM, which further validates the motivation behind our design for the softmax aggregator.

1.3. Iterative Design

We present additional illustrations of the iterative design process with FP-FGNN. Fig. 7 shows examples where a given boundary is initialized with Living room, Master room, Kitchen and Bathroom at arbitrary locations. The floorplans are updated according to the user inputs leading to design of different floorplan layouts from the same boundary. The high fidelity of the predictions along with the good alignment with the boundary given only partial inputs benefits the iterative design process.

1.4. Additional qualitative Results

In this section, we present a series of additional randomly selected floorplans generated by our model, FP-FGNN. Fig. 8 and Fig. 9 show direct output images of FP-FGNN and Fig. 10 and Fig. 11 show the floorplans after post-processing. Alongside each generated floorplan, we provide its corresponding ground truth floorplan to facilitate a comparative analysis of their similarities. The visualized results of this analysis demonstrate that FP-FGNN generates floorplans that bear the closest resemblance to the ground truth ones. Therefore, our model appears to have successfully learned the key features and spatial relationships that underlie the creation of accurate floorplans.

1.5. Implementation Details

Our code is written with Pytorch [24]. We train our model with a learning rate of 0.001, decay rate of 0.0001 along with a step size of 7, hidden dimension of 128 and with batch size of 60. 4 iterations of message passing are performed. We use Adam [13] as the optimizer.

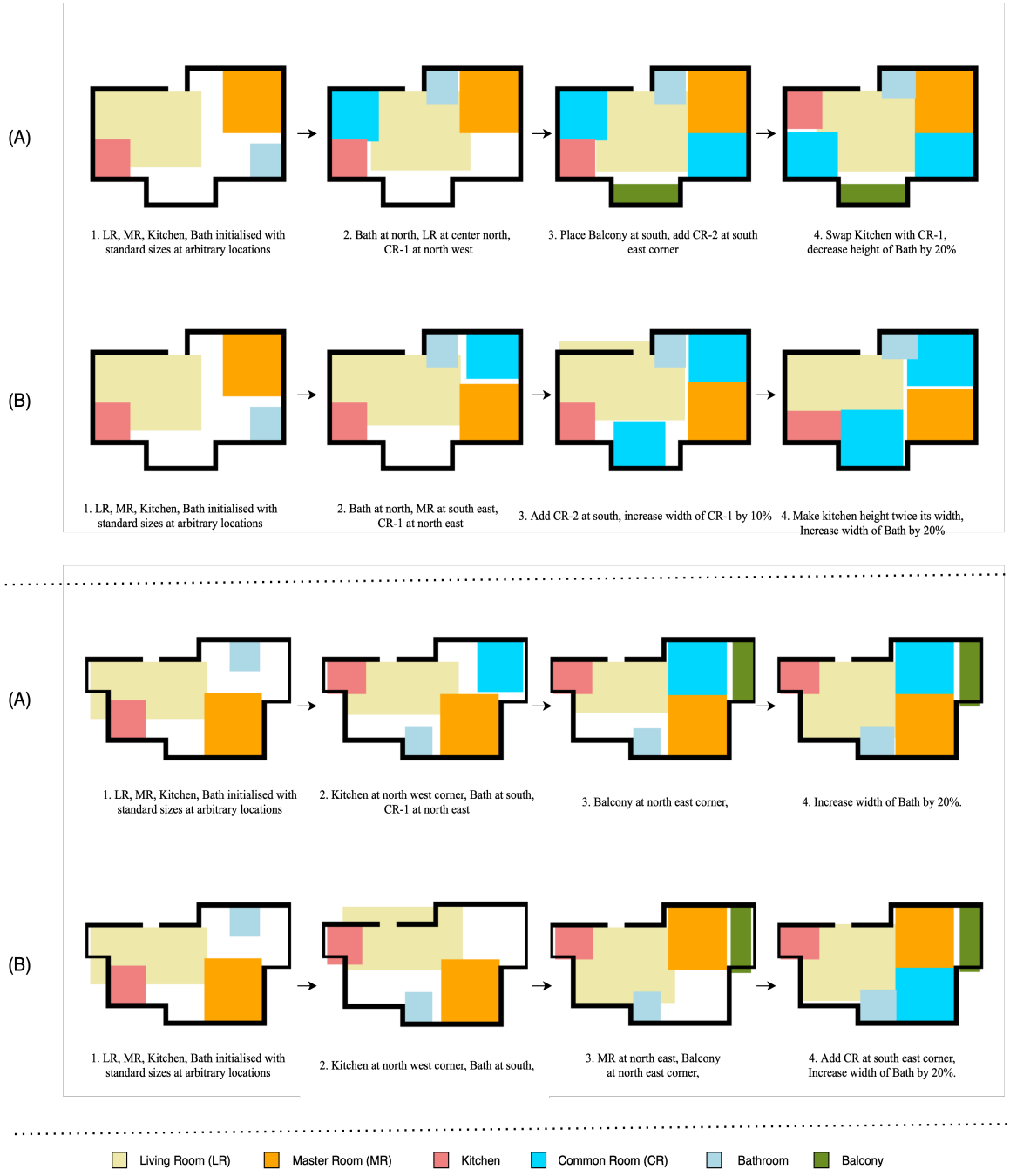

Figure 7. Additional examples showing iterative design process with FP-FGNN

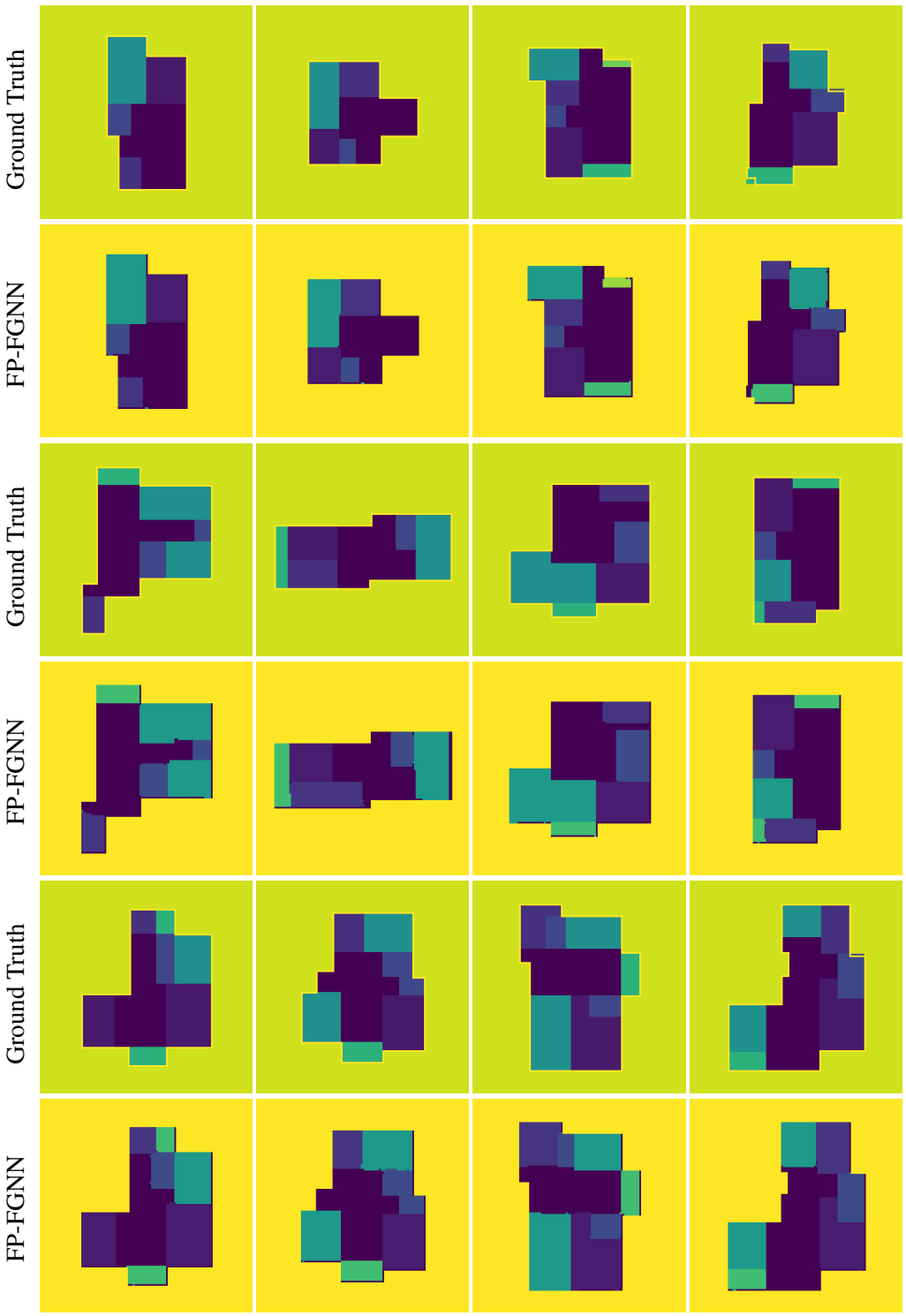

Figure 8. Comparison of floorplans generated by FP-FGNN with the ground truth.

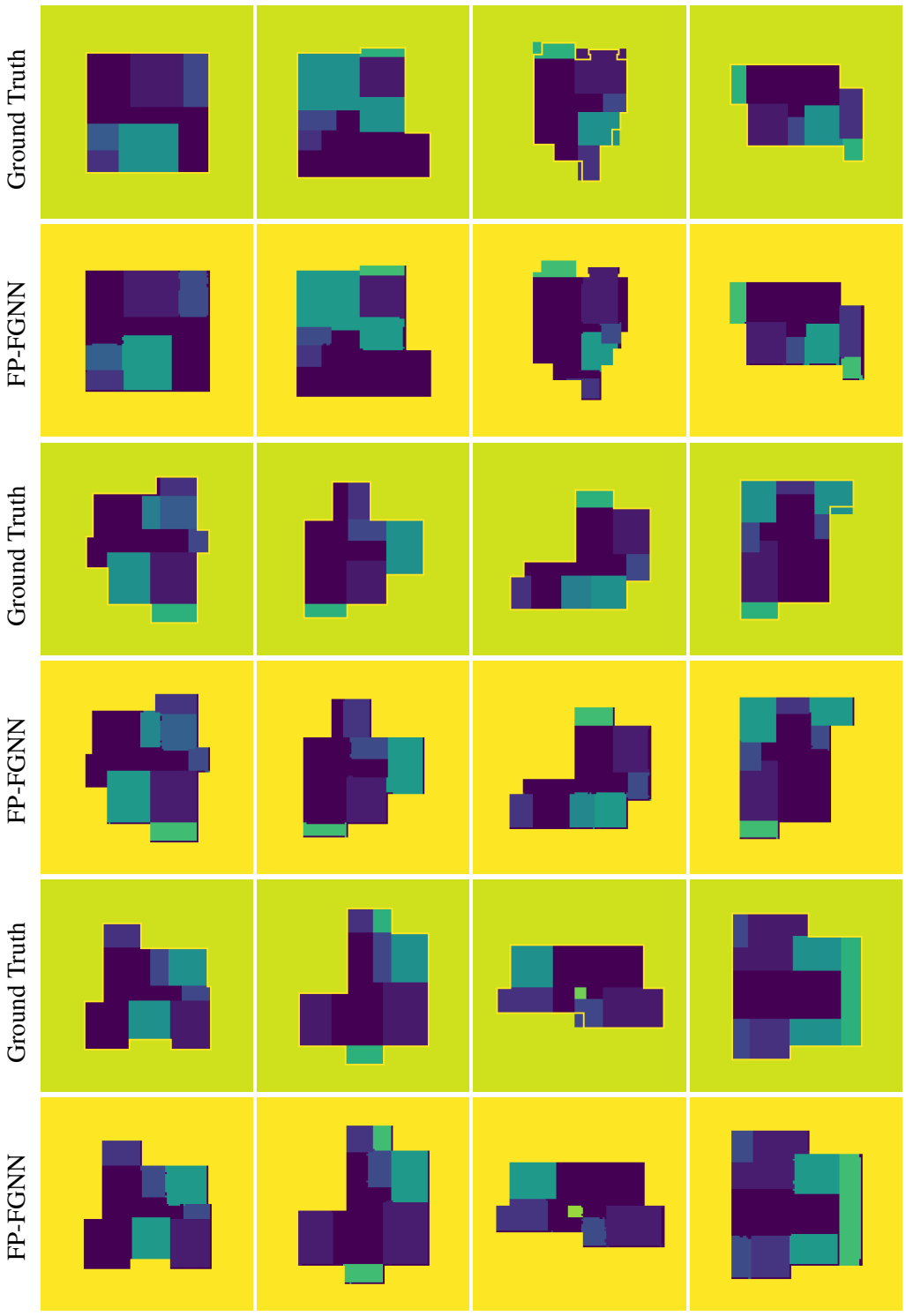

Figure 9. Comparison of floorplans generated by FP-FGNN with the ground truth.

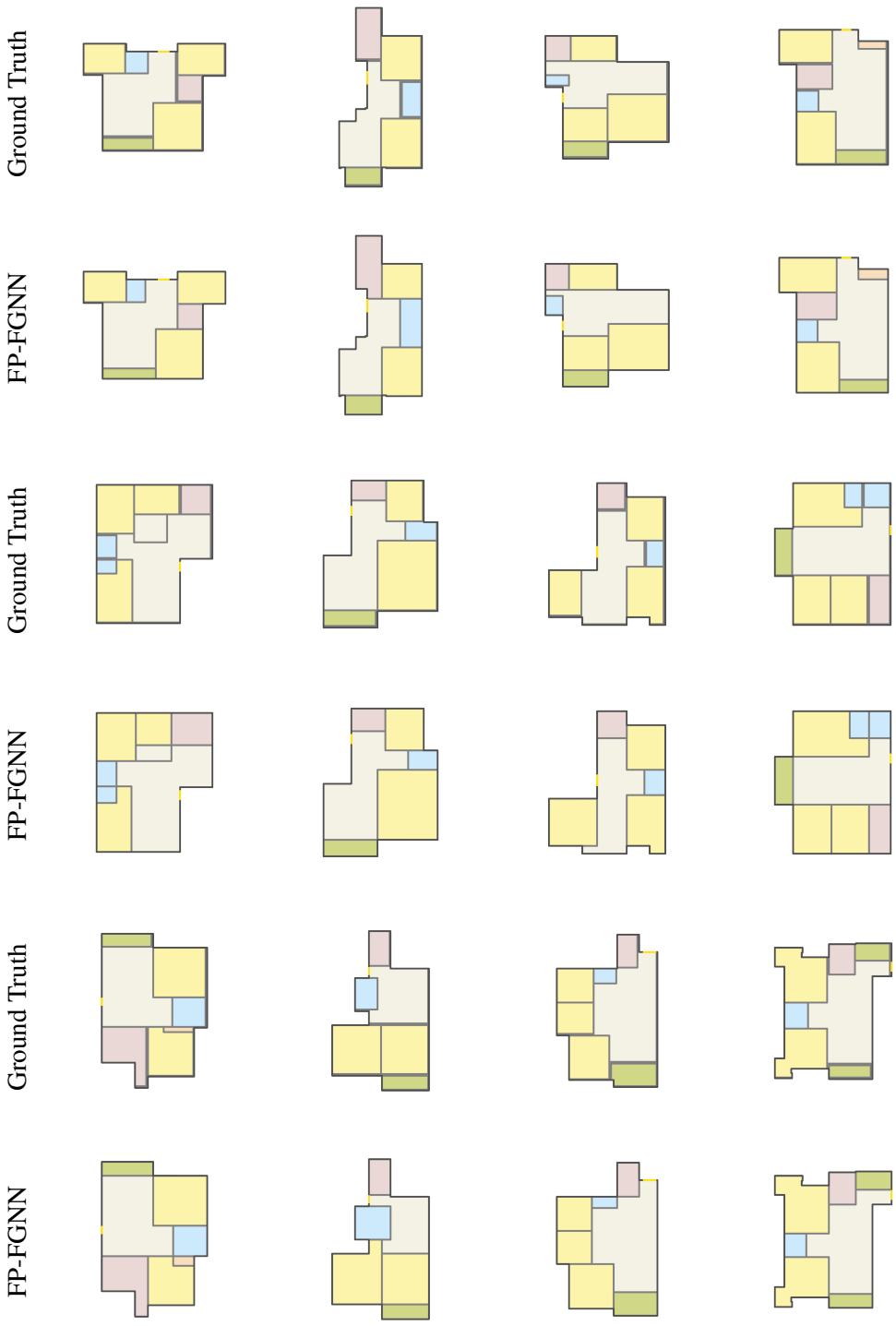

Figure 10. Comparison of floorplans generated by FP-FGNN with the ground truth after post-processing.

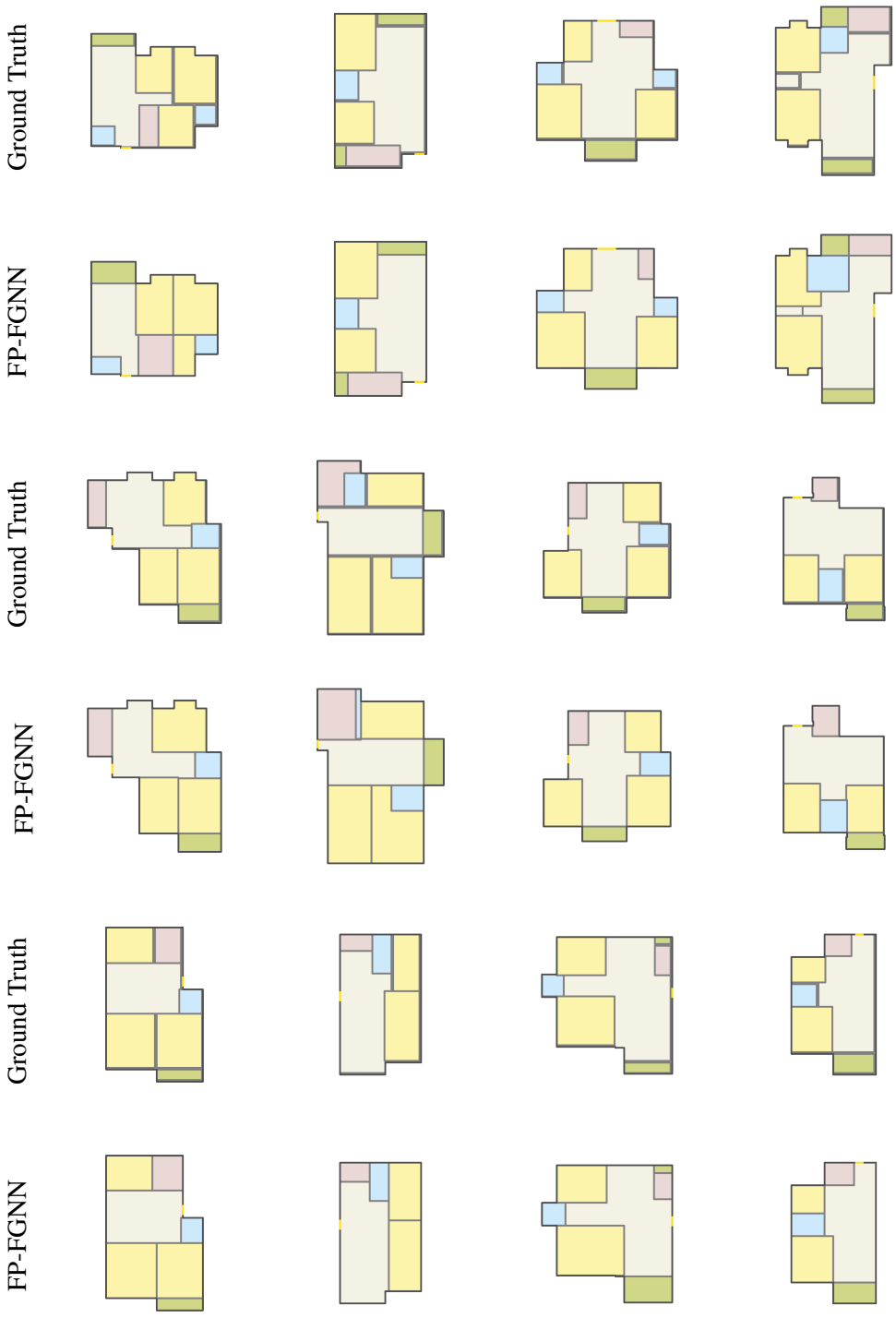

Figure 11. Comparison of floorplans generated by FP-FGNN with the ground truth after post-processing.